Available online at www.sciencedirect.com

SCIENCE DIRECT®

Developmental Biology 269 (2004) 489–504

DEVELOPMENTAL BIOLOGY

www.elsevier.com/locate/ydbio

A proliferative role for Wnt-3a in chick somites

Lisa M. Galli,[a] Karl Willert,[b] Roel Nusse,[b] Zipora Yablonka-Reuveni,[c] Tsutomu Nohno,[d] Wilfred Denetclaw,[a] and Laura W. Burrus[a,*]

[a] *Department of Biology, San Francisco State University, San Francisco, CA 94132, USA*

[b] *Howard Hughes Medical Institute, Department of Developmental Biology, Stanford University School of Medicine, Stanford, CA 94305, USA*

[c] *Department of Biological Structure, University of Washington School of Medicine, Seattle, WA 98195, USA*

[d] *Department of Molecular Biology, Kawasaki Medical School, Kurashiki, Japan*

Received for publication 18 September 2003, revised 23 January 2004, accepted 30 January 2004

Abstract

The proper patterning of somites to give rise to sclerotome, dermomyotome, and myotome involves the coordination of many different cellular processes, including lineage specification, cell proliferation, cell death, and differentiation, by intercellular signals. One such family of secreted signaling proteins known to influence somite patterning is the Wnt family. Although the participation of Wnt-3a in the patterning of dorsal structures in the somite is well established, no clear consensus has emerged about the cellular processes that are governed by Wnt-3a in the somite. The recent demonstration that Wnt-3a has a proliferative role in the neural tube [Development 129 (2002) 2087] suggested that Wnt-3a might also act to regulate proliferation in somites. To test this hypothesis, we first analyzed the effects of Wnt-3a on segmental plate and somite explants (from Hamburger and Hamilton stage 10 chick embryos) grown in culture. These studies indicate that Wnt-3a is capable of maintaining and/or inducing expression of both Pax-3 and Pax-7, transcription factors that have been implicated in proliferation. To directly test for a role in proliferation, explants were immunostained with antibodies against phospho-histone H3. Explants treated with Wnt-3a show an increase in the percentage of cells expressing phospho-histone H3 as compared to controls. To test the proliferative effect of Wnt-3a in vivo, we ectopically expressed Wnt-3a in chick neural tubes via electroporation. Consistent with previous studies, ectopic expression of Wnt-3a in vivo results in a mediolateral expansion of the dermomyotome and myotome. We now show that proliferation of dorsal/dermomyotomal cells is significantly enhanced by ectopic Wnt-3a. Collectively, our explant and in vivo studies indicate that an increase in proliferation plays an important role in the expansion of the dermomyotome and myotome in Wnt-3a-treated embryos. Furthermore, our results demonstrate that small changes in proliferation can dramatically influence patterning and morphogenesis.

Keywords: Wnt-3a; Chick; Explant; Somite; Myogenesis; Dermomyotome; Myotome; Proliferation; Pax-1; Pax-3; Pax-7; MyoD; Myf-5; Myosin heavy chain (MHC); Apoptosis; β-Catenin

Introduction

Somites are the segmented building blocks of the developing trunk that are generated by epithelialization of the segmental plate (for review, see Christ and Ordahl, 1995; Keynes and Stern, 1988; Ordahl et al., 2000). During embryogenesis, somite pairs are formed at a rate of approximately 1 pair/100 min at the anterior end of each segmental plate while cells at the posterior end of the segmental plate are replenished by mitosis and cell ingression during gastrulation. Newly formed somites mature in an anterior to posterior wave such that anterior somites are more mature while posterior somites are less mature. By convention, the most recently formed somite is designated as somite I while more mature somites are numbered in ascending order (Ordahl, 1993). As is the case with the segmental plate, cells in somites I–III are largely uncommitted and undifferentiated. If these somite cells are exposed to a new environment (for instance, by rotating the somite such that the position of the dorsal and ventral halves have been reversed), they will differentiate according to the signals specified by their new environment (Aoyama and Asamoto, 1988; Dockter and Ordahl, 2000). Somites IV–VI exhibit the first signs of differentiation; the delamination of cells to form the ventral mesenchymal sclerotome, which will give

* Corresponding author. Department of Biology, San Francisco State University, 1600 Holloway Avenue, San Francisco, CA 94132. Fax: +1-415-338-2295.

E-mail address: LBurrus@sfsu.edu (L.W. Burrus).

0012-1606/$ - see front matter © 2004 Elsevier Inc. All rights reserved.
doi:10.1016/j.ydbio.2004.01.041

rise to vertebrae and ribs, and the compaction and rotation of the remaining epithelial cells to form the dermomyotome. Subsequent maturation of the dermomyotome into the myotome and dermatome yields skeletal muscle and dermis, respectively. The dorsomedial lip (DML) of the dermomyotome gives rise to the epaxial myotome, which ultimately matures into skeletal muscle of the back (Denetclaw et al., 2001; Ordahl et al., 2001), while the ventrolateral lip (VLL) will generate the hypaxial myotome, which gives rise to body wall and limb muscle (Cinnamon et al., 1999; Denetclaw and Ordahl, 2000).

Embryological studies in the chick and quail have revealed several sources of inductive signals, including the neural tube, notochord, and ectoderm, which are thought to play roles in myotome development (Amthor et al., 1999; Borycki et al., 1998; Brand-Saberi et al., 1993; Buffinger and Stockdale, 1994; Cossu et al., 1996; Dietrich et al., 1997; Fan and Tessier-Lavigne, 1994; Hirsinger et al., 1997; Kenny-Mobbs and Thorogood, 1987; Maroto et al., 1997; Münsterberg and Lassar, 1995; Pownall et al., 1996; Reshef et al., 1998; Rong et al., 1992; Spence et al., 1996; Stern and Hauschka, 1995; Stern et al., 1995; Xue and Xue, 1996). Further experiments suggest that signals from the dorsal neural tube are involved in the patterning of the epaxial, but not the hypaxial myotome (Cossu et al., 1996; Spörle et al., 1996).

As Wnts are known to be potent secreted signaling proteins that are involved in a variety of developmental processes, the expression of *Wnt-1*, *Wnt-3*, and *Wnt-3a* in the dorsal neural tube of developing chick and mouse embryos has generated a substantial amount of interest in their possible roles in the development of the epaxial myotome. As such, it has been shown that ectopic expression of Wnt-1, Wnt-3, or Wnt-3a is sufficient to increase levels of dermomyotomal markers such as *Pax-3* and *Pax-7* (Fan et al., 1997; Maroto et al., 1997; Münsterberg et al., 1995). These Wnt family members, either alone or in combination with Shh, are also able to maintain and/or induce the expression of muscle markers including *MyoD*, *myogenin*, and myosin heavy chain (Capdevila et al., 1998; Münsterberg et al., 1995; Stern et al., 1995; Wagner et al., 2000). Knockout studies performed in the mouse further demonstrate that Wnt-1 and Wnt-3a are required for the establishment of the medial compartment of the dermomyotome. The loss of the medial dermomyotome in these mice is also accompanied by a slight reduction in the levels of *Pax-3* and *Myf-5* transcripts as well as a disorganized myotome (Ikeya and Takada, 1998).

Despite the wealth of data regarding the activities of Wnt-1, Wnt-3, and Wnt-3a in the developing somite, the mechanism(s) by which these Wnts contribute to the formation of the dermomyotome and myotome remains unclear. Do Wnts cause the expansion of the myotome by enhancing myogenesis? Do Wnts act to specify dorsal lineages at the expense of ventral lineages? Do Wnts contribute to the generation of the dermomyotome and the myotome by promoting the proliferation and/or survival of dorsally fated cells? Or do Wnts act by delaying the terminal differentiation of cells in the dermomyotome and myotome? The ability of Wnt-1 and Wnt-3a to enhance proliferation in the neural tube (Megason and McMahon, 2002) led us to hypothesize that Wnt-3a has a proliferative role in somites.

In this paper, we use newly available reagents, including soluble Wnt-3a (Shibamoto et al., 1998; Willert et al., 2003), monoclonal antibodies against Wnt-3a, a Wnt-3a electroporation construct, and antibodies against various somite markers (Bader et al., 1982; Kawakami et al., 1997; Yablonka-Reuveni and Paterson, 2001), to determine whether Wnt-3a does indeed have a proliferative role in chick somite patterning. Wnt-3a dramatically increases the levels of Pax-3 and Pax-7 protein in explant cultures. Wnt-3a also increases cell proliferation in explants while having no effect on cell death. In complementary experiments performed in vivo, the ectopic expression of Wnt-3a throughout the right half of the neural tube by electroporation causes a mild mediolateral expansion of the dermomyotome and a dramatic enlargement of the myotome in adjacent somites 48 h post-electroporation. The expansion of these structures is preceded by an increase in the proliferation dorsal/dermomyotomal cells at 24 h post-electroporation. Cumulatively, our explant and in vivo data suggest that the increase in proliferation of dorsal/dermomyotomal cells drives the mediolateral expansion of the dermomyotome and the myotome.

Materials and methods

Materials

Materials and their respective vendors are as follows: anti-Pax-7 Mab, MF-20 anti-Myosin heavy chain MAb (Developmental Studies Hybridoma Bank); paraformaldehyde (Electron Microscopy Sciences); chick embryo extract, trypsin (Gibco-BRL); fetal bovine serum (Hyclone); α-MEM (Mediatech); goat-anti-mouse IgG (H + L) Cy3, goat anti-mouse IgG (H + L) Cy5, goat-anti-rabbit IgG (H + L) FITC, goat-anti-rabbit IgG (H + L) Cy3 (Jackson Labs); slowfade light antifade kit (Molecular Probes); RT-PCR kit, RNAse-free DNAseI, Rneasy Mini Kit (Qiagen); In Situ Cell Death Detection Kits with fluorescein and Texas methyl red (Roche Biochemicals); insulin, Tyrode's solution (Sigma); anti-β-catenin MAb (BD Biosciences); anti-phospho-histone H3 PAbs (Upstate Technologies); and Sylgard (Dow Corning).

Dr. Charlie Ordahl (UCSF) and Dr. Marianne Bronner-Fraser (Cal Tech) generously provided the anti-Pax-3 MAb while Dr. Sean Megason and Dr. Andy McMahon (Harvard University) were kind enough to share their electroporation construct (pCIG) with us. Dr. Andy McMahon also provided the mouse *Wnt-3a* cDNA while Dr. Rudi Balling donated the quail *Pax-1* cDNA.

DNA subcloning

As the longest available chick Wnt-3a cDNA did not have a signal peptide (Kawakami et al., 2000), we determined the site of the predicted peptide signal cleavage site in both mouse and chick amino acid sequences and appended the cDNA encoding the mouse Wnt-3a signal peptide onto the chick Wnt-3a cDNA. Proper processing of the resultant protein in the endoplasmic reticulum should result in a mature protein that is entirely chick derived (Nielsen et al., 1997).

Preparation and culture of segmental plate and somite explants

Hamburger and Hamilton stage 10 chick embryos (10–12 somites) were harvested and rinsed in Tyrode's solution (Hamburger and Hamilton, 1951). Embryos were pinned onto a Sylgard coated dish (dorsal side up) and lightly treated with trypsin. Using electrolytically sharpened tungsten knives, the posterior end of the segmental plate was dissected away from the neuroepithelium. Moving anteriorly, somites I–VI were also pulled away from the neural tube and notochord. The surface ectoderm was peeled back to expose the segmental plate and somites. These tissues were then dissected away from intermediate mesoderm and pulled-free from the embryo. Growth medium consisted of α-MEM medium supplemented with 15% fetal bovine serum, 2.5% chick embryo extract, 1× penicillin/streptomycin, 4 mM glutamine, and 400 ng/ml insulin. Explants were cultured in equal volumes of growth medium and either control conditioned medium or Wnt-3a conditioned medium (Shibamoto et al., 1998). When using purified Wnt-3a (Willert et al., 2003), explants were cultured in equal volumes of growth medium and control conditioned medium. Equivalent volumes of either control buffer (PBS containing 1 M NaCl and 1% CHAPS, pH 7.3) or purified Wnt-3a were then added to the culture medium. The final concentration of purified Wnt-3a in the assay was 2 nM. Explants were cultured for either 24 or 48 h in humidified 37°C incubators with 5% CO_2. Due to limited quantities of purified Wnt-3a, we were not able to use purified Wnt-3a for all replicates of the explant experiments. All explant experiments were performed at least once with purified Wnt-3a. Indistinguishable results were obtained with Wnt-3a conditioned medium and purified Wnt-3a.

RT-PCR

RNA was purified from explant cultures according to the Rneasy Mini Kit protocol, with the optional addition of DnaseI. RT-PCR was performed according to RT-PCR kit protocol on a GeneAmp PCR System 2400. Control reactions in which either template or the reverse transcription reaction was omitted were performed for every sample. Purified RNA concentration was determined by a spectrophotometer and then the GAPDH products were normalized before using the other primer sets. PCR reactions were subjected to electrophoresis on a 2.5% agarose gel. The following primer sets were used: GAPDH (Dugaiczyk et al., 1983) 5′-AGTCATCCCTGAGCTGAATG-3′ and 5′-AGGATCAACTCCACAACACG-3′, product size 320 bp; Pax-1 5′-GCTGGGTGGTGTCTTCGTGAAC-3′ and 5′-ACTGGTAAAGGGGGTTGTAGGG-3′, product size 452; Pax-3 (Maroto et al., 1997) 5′-TGGAGCCCACCACCACTGTC-3′ and 5′-AACACCAGCTTAACTTGAAG-3′, product size 215 bp; Pax-7 5′-CCAACCACATCCGCCATAAG-3′ and 5′-TCCTCCTCTTCCTCTTTCTTCCC-3′, product size 355 bp; Myf-5 5′-AGGGAACAGGTGGAGAACTA-3′ and 5′-TCATAGCGCCTGGTAGGTCC-3′, product size 340 bp; MyoD 5′-ACTACACGGAATCACCAAATGACC-3′ and 5′-AAGGAATCTGGGCTCCACTGTC-3′, product size 204 bp; MHC 5′-CACAAAAGAACCTGAGAAACACACAAG-3′ and 5′-ATTGCGGGCTTCCTGGATGG-3′, product size 335 bp. RT-PCR experiments were performed a minimum of five times from samples prepared on at least four different dates.

Electroporations

After windowing eggs, India Ink diluted in Tyrode's solution was injected underneath the embryo to enhance visualization. After making a small tear in the vitelline membrane at the site of injection, embryos were overlaid with 1 ml of 1× penicillin/streptomycin diluted in Tyrode's solution. Hamburger and Hamilton stage 11–14 chick embryos were injected in the neural tube at the level of segmental plate with a solution containing DNA (final concentration 1–2 mg/ml), fast green dye (400 ng/ml) and high-viscosity carboxymethyl cellulose (3 μg/ml). Homemade electrodes constructed with 100-μm (diameter) platinum wires that were spaced 4 mm apart were used for the electroporations. Embryos were electroporated with four 50 ms pulses at 30 V with a BTX square wave generator. The embryos were incubated for either 24 or 48 h, harvested and fixed in PBS containing 4% paraformaldehyde for 1–2 h at 4°C. Embryos were washed twice with PBS, incubated in PBS containing 5% sucrose and 0.01% NaN_3 for at least 3 h, and then incubated in PBS containing 15% sucrose and 0.01% NaN_3 overnight. Embryos were then equilibrated in PBS containing 15% sucrose and 7.5% gelatin at 40°C for 1–4 h, oriented at room temperature and then frozen in liquid nitrogen. Serial sections (25–40 μm) were cut on a Leica cryostat.

Immunostaining of explants and tissue sections

Explants were fixed onto slides by fixing for 30 min in PBSMC (PBS with 1 mM $MgCl_2$ and 180 μM $CaCl_2$) containing 4% paraformaldehyde. Slides were then washed twice in PBSMC before immunostaining. For tissue sections, slides were degelatinized by washing in PBS at 50°C

for 10 min and then washed twice in PBS. Slides for both types of experiments were then blocked for 1 h in blocking buffer [3% sheep serum in PBSMC (for explants)/PBS (for sections) with 0.1%Tween]. Slides were incubated in primary antibody diluted in blocking buffer overnight at 4°C and then washed two to four times in PBSMC/PBS plus 0.1% Tween. The slides were blocked for 30 min and incubated in secondary antibody diluted in blocking buffer for 2 h at room temperature. They were then washed four times in PBSMC/PBS plus 0.1% Tween, post-fixed in 4% paraformaldehyde in PBS and mounted in slowfade. Immunostaining of explants with antibody against Pax-3 was performed on two independent samples. All other immunostaining experiments were performed on a minimum of three independent samples.

In situ hybridization of electroporated embryos

Digoxigenin-labeled antisense probe for *Pax-1* was made by transcribing *Xba*I-linearized cDNA with T3 RNA polymerase. Whole-mount in situ hybridizations were performed as previously described (Baranski et al., 2000).

Cell death assay (TUNEL)

For somite explants, the slides were fixed in 4% paraformaldehyde in PBSMC for 1 h at room temperature. For cryostat sections, sections on slides were degelatinized for 10 min in PBS at 50°C before initiating TUNEL protocol. Both sets of slides were washed in PBSMC (for explants)/PBS (for tissue sections) for 30 min at room temperature. The samples were permeabilized in 0.1% Triton X-100, 0.1% sodium citrate for 2 min on ice and washed twice in PBSMC/PBS. The TUNEL reaction mixture was added to the slide and covered in parafilm (for the negative control only the labeling solution was added without the enzyme solution). The slides were incubated in a humidified chamber at 37°C for 1 h, washed three times in PBSMC/PBS, fixed in 4% paraformaldehyde and mounted in Slowfade. Explant cultures were incubated with 100 pg/ml DAPI before fixation. TUNEL analysis was performed on four independent explant samples. For electroporated embryos, we measured apoptosis in 11 sections from two 24 h post-electroporation embryos and 21 sections from two 48 h post-electroporation embryos.

Confocal microscopy

For confocal microscopy, specimens were excited using the 488-nm line of an argon ion laser for visualization of GFP, the 543.1-nm line of a green helium–neon laser for visualization of Cy3, and the 647-nm line of the red helium–neon laser for visualization of Cy5. Fluorescence emission was captured a Nikon E600 Physioscope attached to the Nikon PCM2000 confocal laser scanning unit. Images were collected with 10×, 20×, and 60× objectives. The C-Imaging Simple32 software (Compix, Inc.) controlled the confocal microscope for zeta-axis image acquisitions. Adobe Photoshop version 5.0.2 was used for final image data processing.

Quantitation of proliferation

For explant studies, random fields for the quantitative analysis were chosen with the DAPI filter in place. Representative random fields are shown in Figs. 3A and B. As somites IV–VI demonstrated the least significant increase in proliferation upon addition of Wnt-3a, these images were counted by two investigators. The images were coded before being counted "blind" by one of the investigators. Identical results were obtained by both investigators. The data presented in Fig. 4 represent measurements from a single investigator.

For the analysis of proliferation in vivo, we excluded sections from our data set that had a notochord width/height ratio of over 1.7. As the notochord is a perfectly circular structure (B. Christ, personal communication), the width/height ratio of a true transverse section should be 1.0. It was important to eliminate grossly skewed sections due the segmented nature of somites and the existence of proliferative waves in paraxial mesoderm along the anterior/posterior axis (S. Venters, personal communication). The areas and numbers of proliferative cells were measured by two investigators. For sections derived from embryos that were 24 h post-electroporation, "blind" measurements were performed by one of the investigators. To generate the blind study, the GFP channel was removed from the image and the left/right axis was flipped in nearly half of the images before counting. It was impossible to similarly code sections from embryos that were 48 h post-electroporation as the phenotype was too overt. Both investigators reached identical conclusions. Data shown in Fig. 10 represents the compilation of the measurements of a single investigator (the two sets of data were nearly identical; for the 24-h embryos, we are showing the measurements that were obtained in the "blind" study).

Statistical analysis

Statistical analysis was carried out using the Statistical Analysis System software package (SAS, Cary, NC, version 8.0). Analysis of covariance was performed to determine the significance of treating explant and in vivo samples with Wnt-3a. For the explants experiments, the date that the experiment was performed was considered to be a confounding factor. Although the trend for Wnt-3a-treated explants was always conserved on different dates, there was significant variation in the absolute values. For the in vivo experiments, the embryo from which the data was obtained was included as a confounding factor. Once again, although the trend for Wnt-3a-treated embryos was conserved, there was significant variability among different

embryos (presumably due to slight differences in staging and in expression levels). Pairwise comparisons were performed using Student's *t* test while multiple comparisons were performed using Tukey–Kramer method.

Results

Adjacent tissues are required for the maintenance of marker gene expression

Before testing the role of purified Wnt-3a on explant cultures, we first needed to establish baseline expression levels for dermomyotomal (*Pax-3*, *Pax-7*), myotomal (*Myf-5*, *MyoD*, *MHC*), and sclerotomal (*Pax-1*) markers. Consistent with previously published data (Gerhart et al., 2000; Goulding et al., 1994; Hirsinger et al., 2001; Kiefer and Hauschka, 2001; Maroto et al., 1997; Williams and Ordahl, 1994), our results from RT-PCR indicate that transcripts for *Pax-3*, *Pax-7*, *Myf-5*, and *MyoD* are present in the paraxial mesoderm at all axial levels examined in stage 10 embryos at day 0 of incubation (Fig. 1). *Pax-1* was expressed in somites I–III and IV–VI, but not in the segmental plate (Fig. 1; Barnes et al., 1996; Brand-Saberi et al., 1993; Johnson et al., 1994). As expected, *Myosin heavy chain* transcripts were not detected at any axial levels (Fig. 1). Positive controls in which RNA from HH stage 23 embryos was amplified demonstrated that our *MHC* primers yielded a product of the expected size (data not shown). As it is well documented that adjacent structures are required to maintain expression of these genes in culture (Fan and Tessier-Lavigne, 1994; Maroto et al., 1997; Münsterberg and Lassar, 1995), we performed RT-PCR on explants that had been cultured for 2 days to confirm that we did indeed observe a reduction in the levels of these transcripts. Because slight differences in embryonic stages can show variances in gene expression, samples were paired such that paraxial mesoderm from one side of the embryo was used for day 0 samples while paraxial mesoderm from the contralateral side of the same embryo was used for day 2 cultures. Consistent with results from other groups (Maroto et al., 1997; Münsterberg et al., 1995), we found that *Pax-3*, *Pax-7*, *Myf-5*, and *MyoD* transcripts were substantially diminished after 2 days in culture. *Pax-1* expression exhibited a reproducible slight increase in segmental plate cultures, while it showed a marked decrease in somites I–III and IV–VI. These data confirm the requirement of adjacent tissues for normal expression of somitic markers.

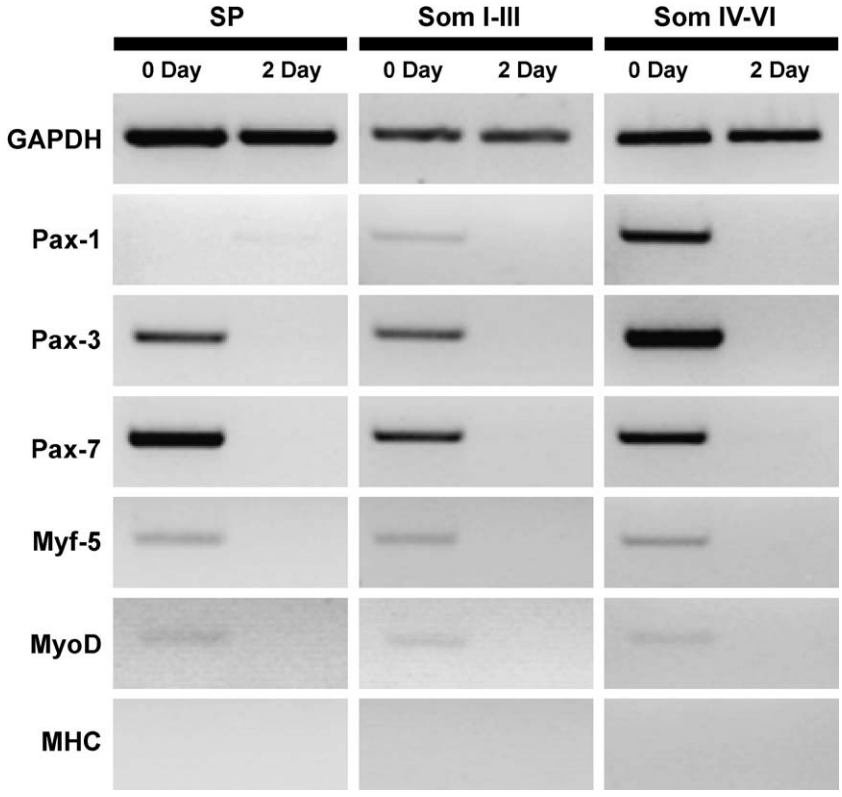

Fig. 1. Tissues adjacent to somites are required for the maintenance of somite marker gene expression in explant cultures. Segmental plate, somites I–III, and somites IV–VI from HH stage 10 embryos were dissected away from all adjacent tissues. Explants from one side of the embryo were immediately frozen in RLT buffer (day 0 samples) while explants from the opposite side of the embryo were cultured for 2 days as described in Materials and methods. Dnase-treated RNA was purified and subjected to RT-PCR using primer sets as indicated. As an internal control, the levels of *GAPDH* were normalized for each pair of samples. Control reactions, in which either template or the RT reaction was omitted, were performed for all samples. These experiments were replicated a minimum of five times from four independently generated samples.

Wnt-3a can maintain and/or induce expression of dorsal somite and myogenic mRNAs

To test the ability of Wnt-3a to maintain and/or induce dorsal somite and myogenic gene expression, we cultured explants in the presence or absence of Wnt-3a for 2 days. Once again, samples were paired such that paraxial mesoderm from one side of the embryo was used for control samples while paraxial mesoderm from the contralateral side of the same embryo was used for Wnt-3a-treated cultures. At all three axial levels tested, the addition of Wnt-3a caused an increase in the levels of *Pax-3*, *Pax-7*, *Myf-5*, and *MyoD* transcripts (Fig. 2). In contrast to data obtained from explant cultures with Wnt-expressing cells (Münsterberg et al., 1995), Wnt-3a had no positive effect on *MHC* levels (Fig. 2). Wnt-3a also had no positive effect on *Pax-1* expression (Fig. 2). Because there is little or no expression of *Pax-1* or *MHC* transcripts after 2 days of culture in the absence of axial structures (Figs. 1 and 2), the ability of Wnt-3a to inhibit *Pax-1* or *MHC* expression was not tested in this experiment. These results demonstrate that Wnt-3a is sufficient to maintain and/or induce the expression of *Pax-3*, *Pax-7*, *Myf-5*, and *MyoD*.

Wnt-3a can maintain and/or induce expression of dorsal somite proteins, but not myogenic proteins

Because transcript levels do not always accurately reflect protein levels, we also immunostained explants for Pax-3, Pax-7 (Kawakami et al., 1997), MyoD (Yablonka-Reuveni and Paterson, 2001), and MHC (Bader et al., 1982). Consistent with our RT-PCR experiments, Pax-3 and Pax-7 were strongly expressed in the nuclei of Wnt-3a-treated explants (Figs. 3A–D).

However, no increase in protein levels was detected for either MyoD or MHC (Figs. 3E–H). Our data contrasts with data obtained from explants with Wnt-1 expressing cells showing that Wnt-1 is able to induce MHC expression (Stern et al., 1995). To confirm our ability to immunostain MyoD and MHC in explant, we cultured somites in the presence of adjacent structures (neural tube, notochord, ectoderm, lateral plate mesoderm) for 48 h and observed robust induction of MyoD and MHC (Fig. 3I). The ability of Wnt-3a to maintain and/or induce *MyoD* transcripts, but not MyoD protein suggests that myogenesis is not the principal effect of Wnt-3a and that additional layers of regulation exist.

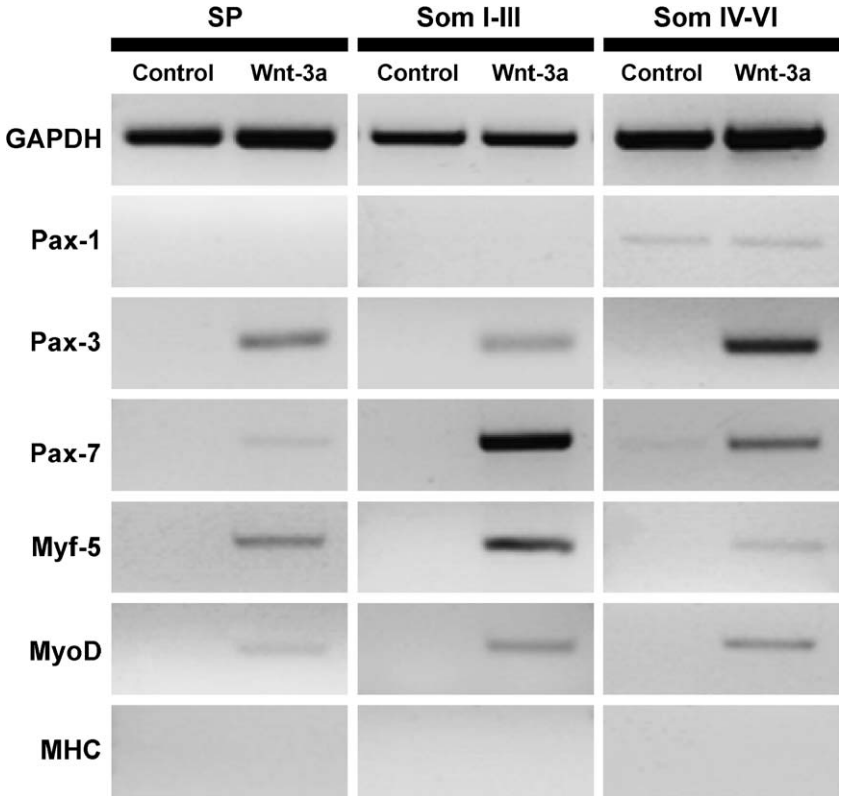

Fig. 2. Wnt-3a maintains and/or induces the expression of dorsal somite and myogenic genes in explant cultures. Segmental plate, somites I–III, and somites IV–VI from HH stage 10 embryos were dissected away from all adjacent tissues. Explants from one side of the embryo were cultured in the absence of Wnt-3a while explants from the contralateral side of the embryo were cultured in the presence of Wnt-3a. Dnase-treated RNA was purified and subjected to RT-PCR using primer sets as indicated. As an internal control, the levels of GAPDH were normalized for each pair of samples. Control reactions, in which either template or the RT reaction was omitted, were performed for all samples. These experiments were replicated a minimum of five times from four independently generated samples.

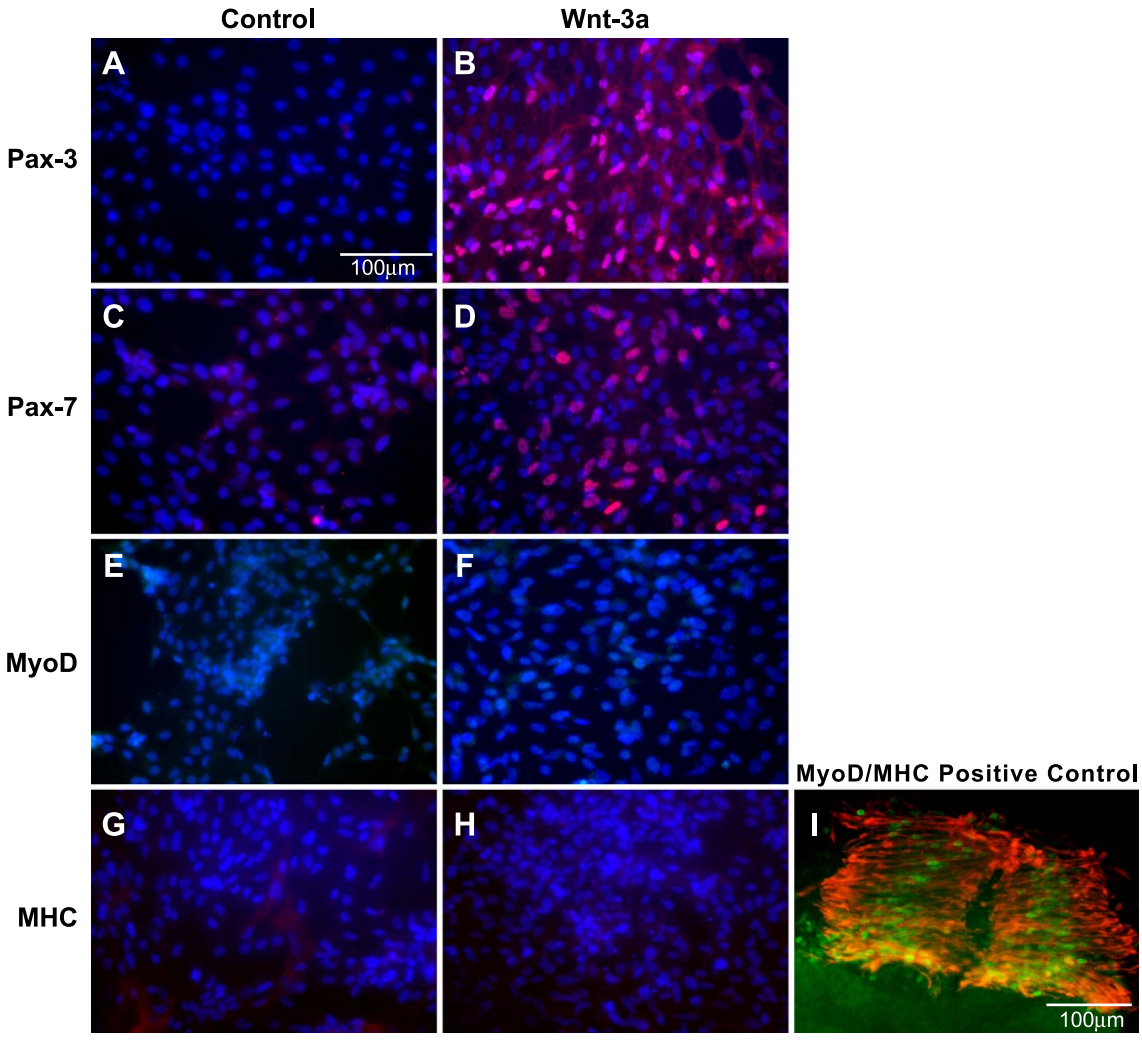

Fig. 3. Wnt-3a maintains and/or induces the expression of Pax-3 and Pax-7 protein, but not MyoD or MHC. Somites I–III from HH stage 10 embryos were dissected away from all adjacent tissues. Explants from one side of the embryo were cultured in the absence of Wnt-3a (A,C,E,G) while explants from the contralateral side of the embryo were cultured in the presence of Wnt-3a (B,D,F,H). As a positive control for MyoD and MHC immunostaining, somite explants were cultured in the presence of all adjacent structures, including ectoderm, neural tube, notochord, and lateral plate mesoderm (I). Explants were grown on gelatin coated eight-well microscope slides before immunostaining with the designated antibodies. Pax-3, Pax-7, and MHC immunolabeling was detected with Cy3 conjugated secondary antibodies while MyoD was detected with FITC-labeled secondary antibody. Nuclei were counterstained with DAPI. Merged images are shown for DAPI and either Pax-3, Pax-7, MyoD, or MHC (A–H). For the positive control, a merged image of MyoD and MHC immunostaining is shown (I). Immunostaining with Pax-3 antibodies was performed on two independent samples while immunostaining with all other antibodies was performed on a minimum of three independent samples.

Surprisingly, we sometimes detected cells with very faint MHC expression in control explants (Fig. 3G), but not in Wnt-3a-treated explants (Fig. 3H). These cells were morphologically distinct from MHC positive cells that arise from coculturing somites with adjacent tissues (Fig. 3I) and did not express MyoD (data not shown). Whereas the results with Pax-3, Pax-7, and MyoD were highly reproducible, this population of MHC positive cells was only detected in four out of seven experiments. These results raise the possibility that Wnt-3a is capable of repressing the differentiation of a subpopulation of myogenic cells and are consistent with the ability of Wnt-3a to repress terminal differentiation of muscle in wing bud micromass cultures (Anakwe et al., 2003).

To determine if the responsiveness of explants is dependent on the axial level from which the tissue was derived, we cultured segmental plate, somites I–III and somites IV–VI in the presence or absence of Wnt-3a and determined the percentage of Pax-7-positive nuclei. Preliminary immunohistochemical analysis of HH stage 10 embryos has shown that Pax-7 protein appears to be present in virtually all cells in the somite at the level of somite I and restricts to approximately 90% of the cells by somite VI (data not shown). Consistent with the loss of *Pax-7* transcripts in the absence of adjacent structures, Pax-7 protein was completely absent in control cultures. Whereas 26% of the Wnt-3a-treated cells at the level of segmental plate express Pax-7, 52% and 47% of the cells at the level of somites I–III and

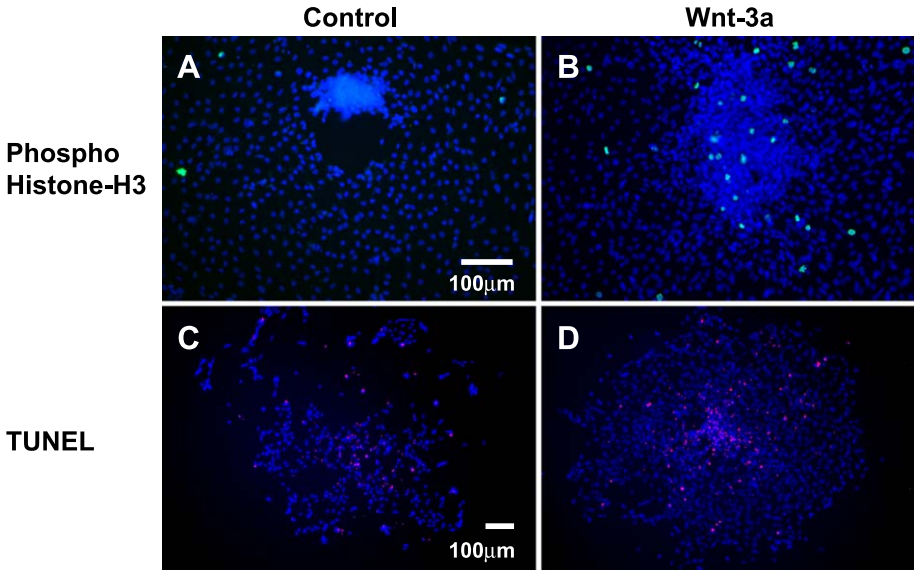

Fig. 4. Wnt-3a promotes proliferation, but does not affect apoptosis in explant somite cultures. Somites I–III from HH stage 10 embryos were dissected away from all adjacent tissues. Explants from one side of the embryo were cultured in the absence of Wnt-3a (A,C) while explants from the contralateral side of the embryo were cultured in the presence of Wnt-3a (B,D). After 2 days of culture on gelatin-coated slides, explants were either immunostained with antibodies against phospho-histone H3 (with Cy3 conjugated secondary; A,B) or subjected to TUNEL analysis (detected with Texas Red; C,D). Nuclei were counterstained with DAPI. Details pertaining to quantitation are in Materials and methods. Whereas a significant increase in the presence of mitotic cells is observed in Wnt-3a-treated cultures, no difference in the number of apoptotic fragments was detected.

IV–VI, respectively, expressed Pax-7 (n = 8; data not shown). These data indicate that somites I–III and IV–VI are mildly more responsive than segmental plate ($P < 0.01$ for multiple comparison analysis). Interestingly, not all Wnt-3a-treated cells express Pax-3 or Pax-7 (Figs. 3A–D) although doses of Wnt-3a that cause maximal induction of β-catenin in an L cell assay were used (data not shown; manuscript in preparation). We do not know if the inability of Wnt-3a to maintain and/or induce protein expression in the same percentage of cells as observed in wild-type somites reflects the normal restriction of Pax-3 and Pax-7 expression over a 48-h time period in vivo or if it is a by-product of the culture system.

Wnt-3a stimulates proliferation, but does not alter apoptosis, in explant cultures

Two observations compelled us to examine proliferation and apoptosis in Wnt-3a-treated cultures. First, Pax-3 activity is correlated with proliferation, inhibition of differentiation, and/or cell survival in a variety of systems (Amthor et al., 1999; Borycki et al., 1999; Epstein et al., 1995; Mennerich and Braun, 2001). Additionally, Wnt-3a-treated explants were clearly larger than control explants. Cumulatively, these data suggested that treatment with Wnt-3a cause either an increase in cell size, an increase in proliferation, a decrease in differentiation, a decrease in apoptosis, or some combination thereof. Wnt-3a-treated explants indeed had significantly more DAPI-labeled nuclei, suggesting that the increase in the area of the explanted tissue was due to the presence of additional cells and not merely an increase in cell size. To test for a possible increase in proliferation, we immunostained explants with anti-phospho-histone H3, which labels cells in M phase (Hendzel et al., 1997; Wei et al., 1999). Immunostaining of cultures with anti-phospho-histone H3 revealed a statistically significant ($P < 0.0001$) enhancement of the percentage of cells undergoing proliferation at all three axial levels (Figs. 4A–B and 5). Consistent with results obtained for the

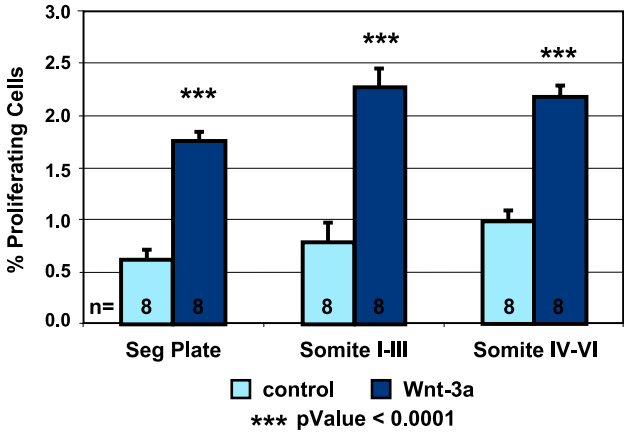

Fig. 5. Wnt-3a increases the percentage of proliferative cells in the segmental plate, somites I–III and somites IV–VI of HH stage 10 embryos. We quantitated the effects of Wnt-3a on proliferation by calculating the percentage of phospho-histone H3 positive cells in the absence or presence of Wnt-3a. Explants were cultured for either 24 or 48 h before immunostaining. These data represent cells counts from eight randomly chosen fields (n = 8; 20× objective; each field contained approximately 1000 cells) from four separate experiments.

maintenance and/or induction of Pax-7 expression, the segmental plate is less responsive to Wnt-3a than somites I–III and IV–VI. However, this difference is less significant ($P < 0.2$) than observed for Pax-7 ($P < 0.01$). We also analyzed apoptosis using terminal deoxynucleotidyl transferase mediated dUTP nick end labeling (TUNEL). Quantitation of apoptotic fragments revealed no significant difference between control and Wnt-3a-treated explants (Figs. 4C–D). Together, these data demonstrate that Wnt-3a increases proliferation in segmental plate and somites I–VI, but does not alter apoptosis.

Ectopic Wnt-3a protein is detected close to the site of synthesis in vivo

To confirm and extend our results in vivo, we ectopically expressed Wnt-3a in the neural tube via electroporation. We chose to electroporate the neural tube rather than somites because we reasoned that ectopic expression of Wnt-3a in the neural tube would more closely mimic normal Wnt-3a signaling. Electroporations resulted in the expression of GFP in the neural tube from the level of the forelimb to the level of the hindlimb (Figs. 6A,E). The presence of Wnt-3a protein was confirmed at 24 h (Figs. 6A–D) and 48 h (Figs. 6E–H) post-electroporation by immunostaining with anti-Wnt-3a MAbs developed in our laboratory (manuscript in preparation). Under the conditions used in these experiments, these antibodies do not recognize endogenous Wnt-3a. Due to the presence of the IRES sequence in the electroporation construct (Megason and McMahon, 2002), the Wnt-3a protein and nuclear targeted GFP were independently translated. As expected, Wnt-3a protein was visualized in cells that were also expressing GFP. While Wnt-3a is robustly expressed at 24 h post-electroporation, its levels appear to decrease relative to GFP by 48 h post-electroporation, suggesting that Wnt-3a protein does not perdure as long as GFP. Consistent with the localization of Wnt proteins in COS cells (Burrus and McMahon, 1995), bright immunostaining around the perimeter of the nucleus suggests the presence of Wnt-3a protein in the endoplasmic reticulum/secretory pathway. However, we did not detect any Wnt-3a protein diffusing away from the site of synthesis. This could indicate that Wnt-3a acts over very short distances or that the antibody epitope on secreted Wnt-3a is

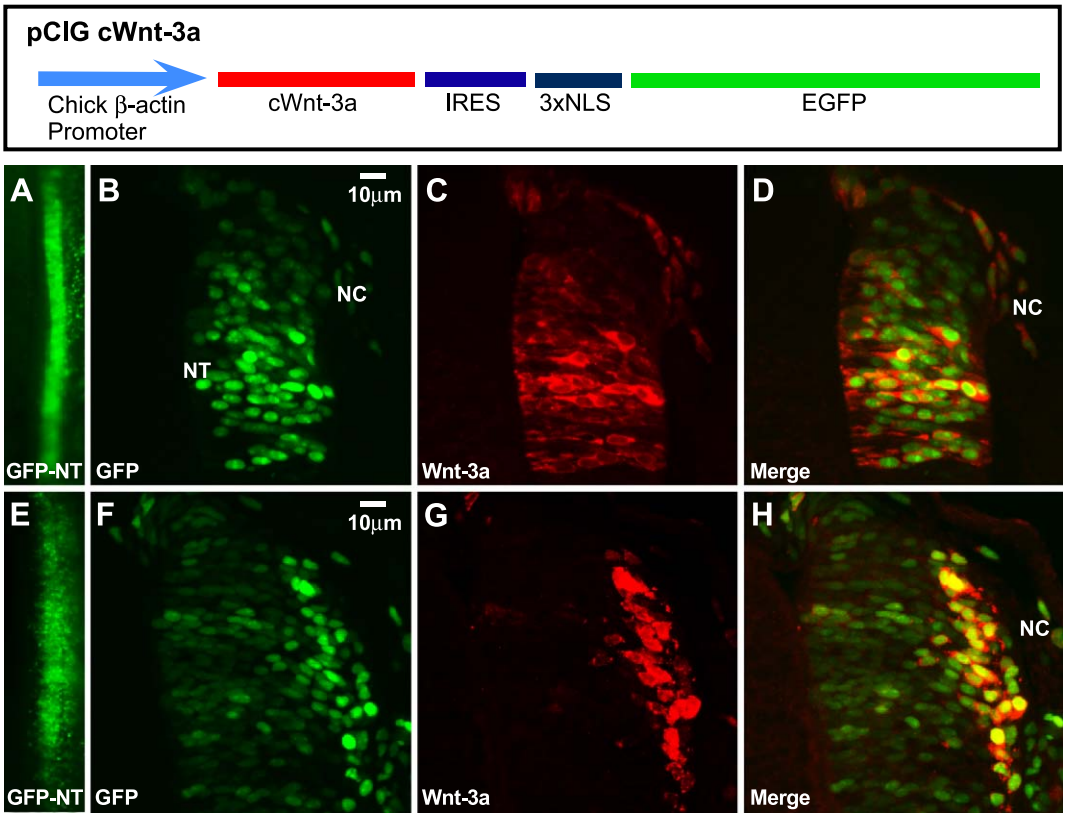

Fig. 6. Ectopic expression of chick Wnt-3a. A diagram depicting the salient elements of the Wnt-3a expression construct is shown (top). The chick β-actin promoter is used to drive the expression of a bicistronic mRNA, which contains the Wnt-3a coding sequence followed by an internal ribosome entry sequence (IRES) and eGFP with a nuclear localization sequence (NLS). HH stage 11–14 embryos were injected in the neural tube at the level of the segmental plate before electroporation. Electroporated cells are marked by the expression of GFP. Expression typically extends from the level of the forelimb to the level of the hindlimb. A dorsal view of embryos at 24 h (A) and 48 h (E) post-electroporation is shown. The localization of GFP to the nucleus is seen in transverse sections through the neural tube (B,F). Electroporated cells are present in the right half of the neural tube as well as in migrating neural crest (B,F). Immunostaining with antibodies directed against Wnt-3a demonstrates the co-expression of Wnt-3a (C,G). NC = neural crest; NT = neural tube.

masked. In addition to ectopic expression in the neural tube, we often observed expression in migrating neural crest cells (Figs. 6D,H).

Ectopic expression of Wnt-3a causes a mediolateral expansion of the dermomyotome and the myotome

To determine the effect of ectopic Wnt-3a on somite patterning, we immunostained for Pax-3, Pax-7, MHC, and MyoD. Consistent with previous results (Megason and McMahon, 2002), we see a ventral expansion of both Pax-3 and Pax-7 in the electroporated side of the neural tube (Figs. 7C–D). We also see a kink in the ventral neural tube, which is presumably caused by the increase in proliferation (Figs. 7C–F; Megason and McMahon, 2002). At 48 h post-electroporation (HH stage 21–22), comparison of the experimental side of the embryo to the control side of the embryo demonstrated a 1.15-fold increase in area demarcated by Pax-3 and Pax-7 expression in the dermomyotome (Figs. 7C–D and 8). Although not visually obvious, we have documented this increase in the area of the dermomyotome by careful quantitation (Fig. 8). We also found that the area of MyoD and MHC expression in the myotome was noticeably expanded on the experimental side (Figs. 7E–F). Quantitative measurements confirm a 1.82-fold increase in the size of the myotome (Fig. 8). In previous experiments in which Wnt-3a-expressing cells were injected directly into somites, the myotome was greatly enlarged and had altered morphology (Wagner et al., 2000). By contrast, we observe an enlarged, but otherwise normal looking myotome. It is likely that this difference can be ascribed to the different methods of introducing Wnt-3a or the expression of additional factors by the Wnt-3a-expressing cells.

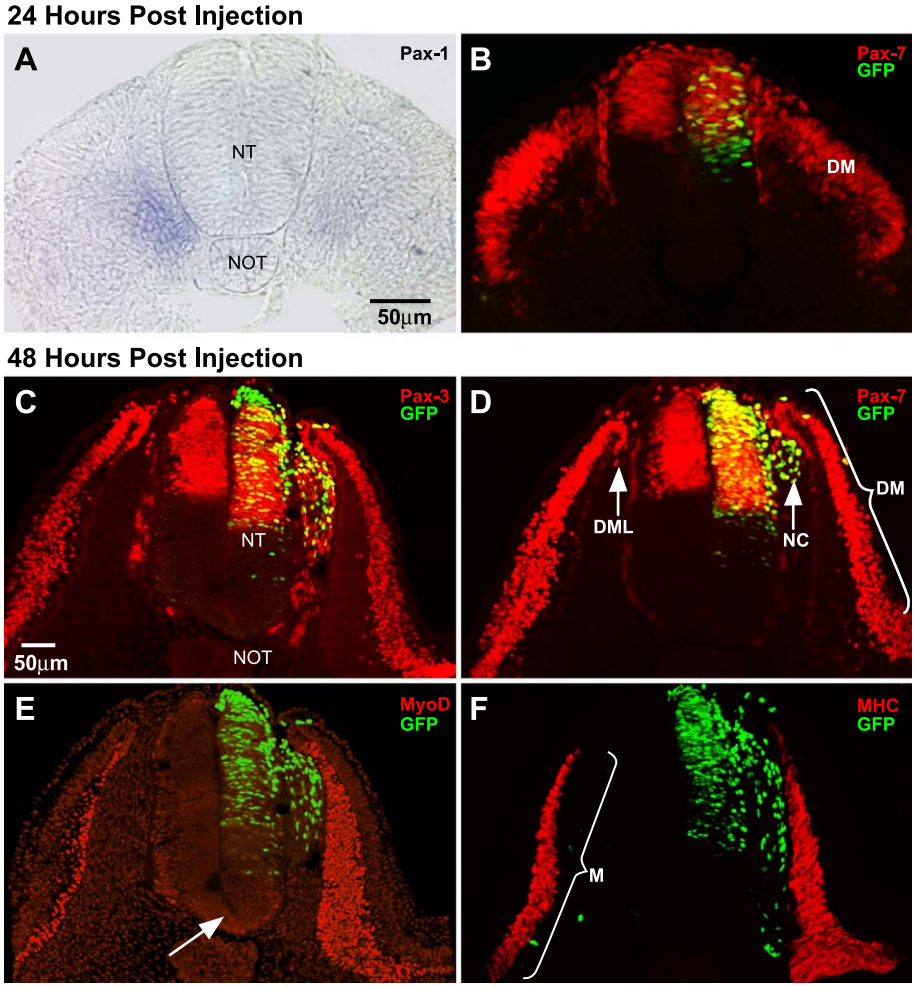

Fig. 7. Analysis of gene/protein expression in embryos that are ectopically expressing Wnt-3a. Embryos were subjected to in situ hybridization (A) or antibody immunolabeling (B–F) either 24 h (A,B) or 48 h (C–F) post-electroporation. At 24 h post-electroporation (HH stage 16–17), the ectopic expression of Wnt-3a causes a reduction of *Pax-1* expression as compared to the control side of the embryo (A). However, Pax-7 expression does not exhibit a commensurate expansion (B). At 48 h post-electroporation (HH stage 21–22), Pax-3 (C) and Pax-7 (D) mark the domain of the dermomyotome, which is slightly expanded in response to Wnt-3a. The myotome, which is marked by immunostaining with antibodies against MyoD (E) and MHC (F), is substantially enlarged in response to Wnt-3a. The arrow in E points to the kink in the neural tube. DM = dermomyotome; DML = dorsomedial lip; M = myotome; NC = neural crest; NOT = notochord; NT = neural tube.

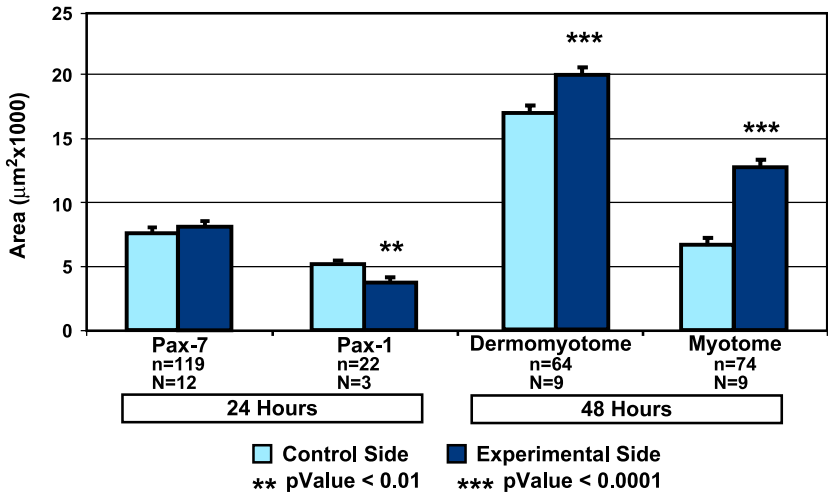

Fig. 8. The loss of ventral cell fates precedes the expansion of dorsal cell fates. To quantitate the change in the gene/protein expression patterns in the somite, we measured the areas of expression in multiple transverse sections. While the reduction of the *Pax-1* expressing area is significant ($P < 0.01$) at 24 h post-electroporation, there is no significant increase in the size of the Pax-7-expressing domain. However, by 48 h post-electroporation, the dermomyotome and the myotome are both significantly increased in size. N = number of embryos; n = number of sections.

The following experiments were conducted to help us distinguish which cellular processes are responsible for the Wnt-3a-induced expansion of the dermomyotome and the myotome. First, to test for a possible role in lineage specification, we extended our analysis of the expression of sclerotomal, dermomyotomal, and myotomal markers in embryos 24 and 48 h post-electroporation. In 24-h embryos (HH stage 16–17), we see a significant loss of *Pax-1* mRNA expression, but no significant expansion of Pax-7 protein expression (Figs. 7A–B and 8). Thus, at this early time point, it does not appear as though a simple lineage switch of ventral to dorsal cell fates has occurred. In contrast, embryos cultured for 48 h post-electroporation (HH stage 21–22) have expanded domains of expression for both dermomytomal and myotomal markers (Figs. 7C–F and 8) while continuing to exhibit a diminished domain of *Pax-1* expression (data not shown).

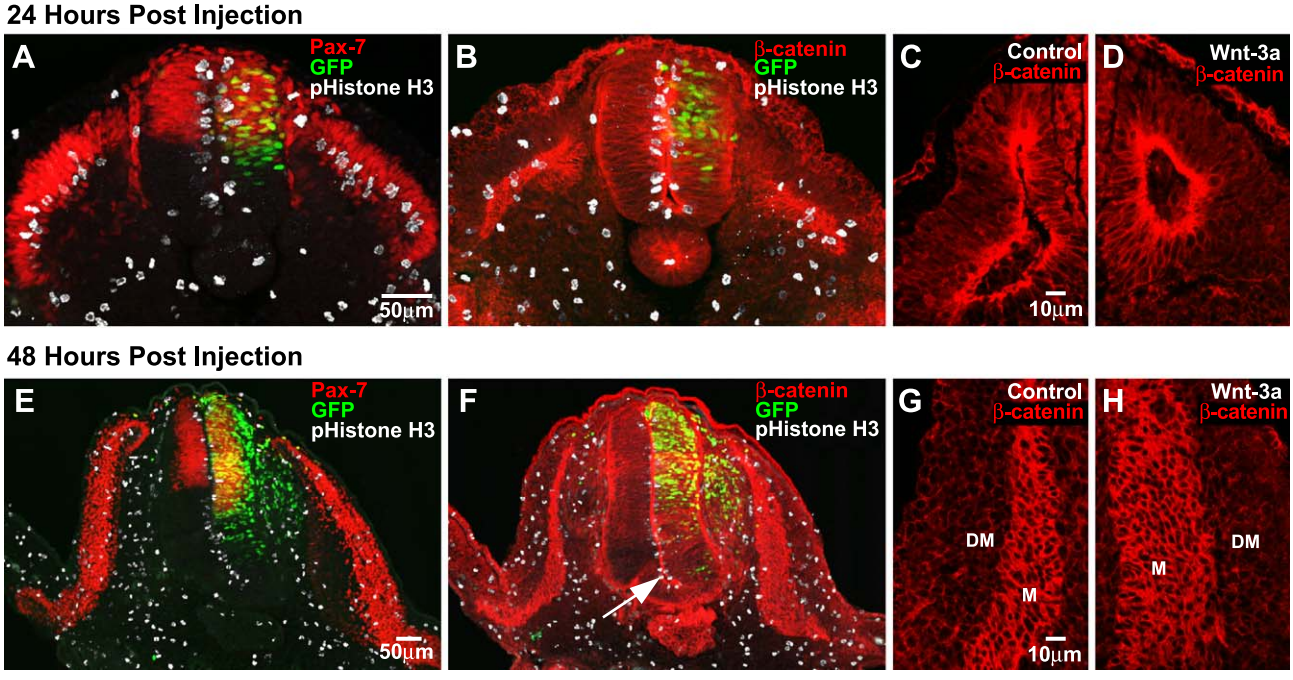

Fig. 9. Wnt-3a has a proliferative effect on somite cells. To assess the role of proliferation, transverse sections from embryos at both 24 h (A,B) and 48 h (E,F) post-electroporation were immunostained with anti-phospho-histone H3 antibodies and either Pax-7 or β-catenin antibodies. Immunostained sections were analyzed by confocal microscopy. High-magnification images of β-catenin staining (C,D,G,H) were used to determine cell areas. The arrow in F points to the characteristic kink in the neural tube.

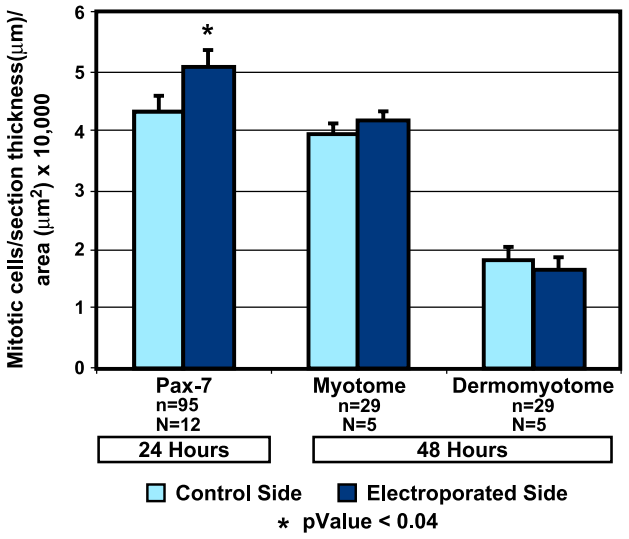

Fig. 10. An increase in proliferation precedes the expansion of dorsal cell fates. To examine the role of proliferation in the expansion of dorsal cell fates, electroporated embryos were immunostained with anti-phospho-histone H3 antibodies and either Pax-7 or β-catenin antibodies. At 24 h post-electroporation, cells in mitosis were counted in the Pax-7-positive region. At 48 h post-electroporation, mitotic cells were counted in either the dermomyotome (as indicated by Pax-7) or the myotome (as indicated by β-catenin). Because the thickness of our sections was slightly variable, we first normalized our data back to section thickness. We then normalized data to the area of the region we were measuring. Additional details pertaining to quantitation are in Materials and methods. N = number of embryos; n = number of sections.

To examine the role of proliferation in the expansion of the dermomyotome and myotome, we immunostained sections from electroporated embryos with anti-phospho-histone H3 antibodies (Hendzel et al., 1997). We chose to immunostain with these antibodies rather than assaying for the incorporation of BrdU as the incorporation of BrdU into the genome has been found to affect MyoD gene expression (Tapscott et al., 1989). To specifically address proliferation in dorsal/dermomyotomal cells of 24 h embryos, we co-immunostained with Pax-7. To assess proliferation in the dermomyotome and myotome of 48 h embryos, we co-immunostained with either Pax-7 or β-catenin. Whereas Pax-7 immunolabeling demarcated the dermomyotome, β-catenin immunolabeling outlines all cells and allowed us to easily count proliferative cells in the myotome. Although our β-catenin immunostaining effectively labeled the plasma membrane of cells, we did not detect the accumulation of nuclear β-catenin in response to Wnt-3a (Figs. 9C,D,G,H). We found that there was indeed an increase in number of proliferative cells in both the dermomyotome (Figs. 9A,E) and the myotome (Fig. 9F) of the experimental side of the embryo as compared to the control side (and to embryos electroporated with empty vector). For the 48-h embryos, this result was not unexpected as larger structures with more cells would be expected to have commensurately more proliferative cells. To account for possible differences in cell numbers, we normalized our data back to the area of the Pax-7- and β-catenin-expressing domains. This means of normalization is only valid if the density of the cells, and hence the size of the cells, is unchanged. To determine whether the cell size was indeed unchanged, we measured the average area of cells at both 24 and 48 h by using β-catenin immunolabeling to outline cells (Figs. 9C,D,G,H). At 24 h post-electroporation, we observe no change in the size of Pax-7-expressing cells on the electroporated side of the embryo as compared to the contralateral side (Figs. 9C,D). When we then divide the number of proliferative cells by the area of the Pax-7 domain, we find that there is indeed a statistically significant 1.18-fold increase in the proliferation of these cells ($P < 0.04$; Fig. 10). Further analysis shows that this significant increase in proliferation is observed in immature somites that are largely epithelial in nature as well as in more mature somites that have already formed myotomes (data not shown). Control experiments in which embryos were electroporated with empty vector (pCIG alone) reveal no statistically significant differences in proliferation between the experimental and control sides of the embryos at 24 h post-electroporation (data not shown). By 48 h post-electroporation, there is no statistically significant

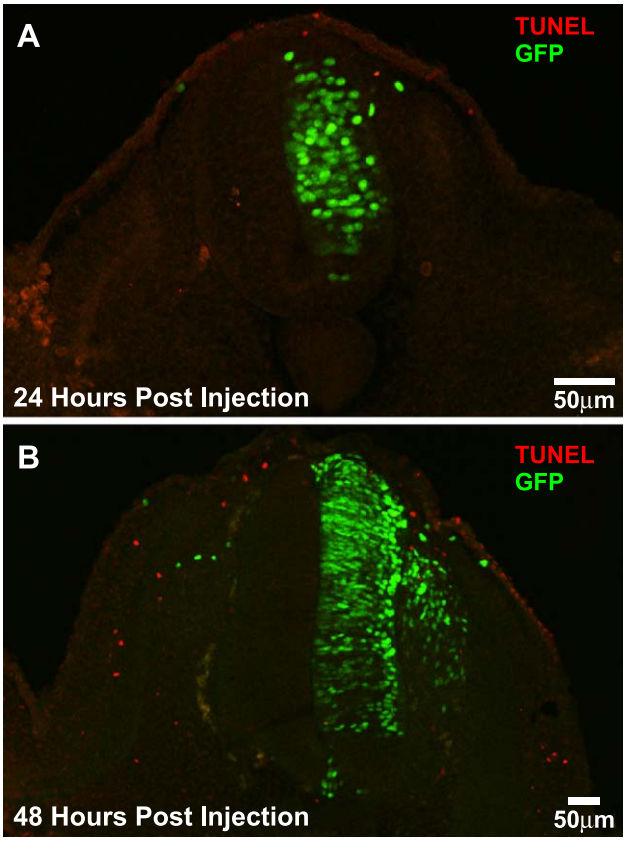

Fig. 11. Wnt-3a does not affect cell survival in somites of electroporated embryos. TUNEL analysis was performed on embryos at 24 h (A) and 48 h (B) post-electroporation to assess apoptosis. Although an edge effect was sometimes observed in the ectoderm, quantitation of apoptotic fragments in the somites revealed no quantitative differences between electroporated and control sides of the embryo.

change in proliferation in either the dermomyotome or the myotome. It is possible that this result is a reflection of the decline of ectopic Wnt-3a expression over time or the increased distance between the neural tube and the bulk of the dermomyotome/myotome over time. Interestingly, when we examined cell size in 48 h embryos (HH stage 21–22), we found that the size of the myotomal cells on the Wnt-3a-treated side of the embryo was 1.13-fold larger than on the control side ($P < 0.01$) while the size of the dermomytomal cells was unchanged (Figs. 9G,H). Consistent with the results from our explant studies, these data suggest that the observed increase in proliferation in dorsal/dermomyotomal cells in 24-h embryos precedes the formation of the dermomyotome and myotome and significantly contributes to the expansion of these structures in Wnt-3a-treated embryos.

Lastly, we tested for Wnt-3a-induced changes in apoptosis. Our TUNEL analysis revealed that there is very little apoptosis occurring in pCIG control embryos (data not shown), suggesting that a diminution of the levels of apoptosis would be insufficient to account for the expansion of the dermomyotome and myotome. Consistent with this line of reasoning, TUNEL analysis revealed no differences in apoptosis between the control and experimental sides of embryos electroporated with the Wnt-3a construct (Figs. 11A,B).

Discussion

In this paper, we have demonstrated a clear proliferative role for Wnt-3a both in explant cultures and in vivo. In explants, Wnt-3a causes an increase in the percentage of proliferative cells at all axial levels. Consistent with these data, ectopic expression of Wnt-3a in the neural tube of chick embryos causes a statistically significant increase ($P < 0.04$) in the percentage of proliferating cells in the region marked by Pax-7 expression in both immature and mature somites at 24 h post-electroporation. This increase in the proliferation of dorsal/dermomyotomal cells occurs before the expansion of the dermomyotome and myotome. Although a 1.18-fold increase in proliferation is fairly subtle, the effect of increasing proliferation by this amount over the course of three 9–10 h cell cycles during the peak expression period (Primmett et al., 1989) would increase the number of cells by a factor of 1.64 (1.18^3). If one also takes into account the fold increase in the area of the myotomal cells, which is 1.13-fold, these calculations predict a 1.85-fold (1.64×1.13) expansion of the myotome. This is almost precisely what was observed. While there are several sources of variability that have not been accounted for in these calculations, they demonstrate that subtle differences in proliferation can have substantive effects on the size of a structure. These data are consistent with reported proliferative effects of Wnt protein in the developing neural tube and limb. In the neural tube, ectopic Wnt-3a expression causes a 1.1-fold to 2-fold increase in proliferation depending on the region analyzed (Megason and McMahon, 2002) while in the limb, loss of Wnt-5a activity results in a 1.15-fold loss of proliferation and is accompanied by a failure of limb outgrowth (Yamaguchi et al., 1999). Likewise, Miller et al. have performed exhaustive studies, which show that extremely small changes in proliferation have dramatic effects on the patterning of various structures in the developing chick (Miller, 1982; Miller and Olcott, 1989; Miller et al., 1993, 1994, 1999).

While the timing and amplitude of the proliferative effect are consistent with proliferation being the primary effect of Wnt-3a, we have considered many other mechanisms of action. For instance, if the expansion of dorsal structures were due to a conversion of ventral to dorsal lineages, we would expect that the loss of Pax-1 expression would be accompanied by an expansion of Pax-3 and/or Pax-7 expression. Consistent with the observations of Capdevila et al. (1998) and Ikeya and Takada (1998), we do not observe this. Likewise, if the primary role of Wnt-3a was to promote myogenesis, we would expect that Wnt-3a would be able to induce the expression of MyoD (and possibly MHC) protein. Although we do see an increase in *Myf-5* and *MyoD* transcripts in explant experiments, we observe no induction of MyoD or MHC proteins. As Pax-3 has been shown to be indirectly upstream of MyoD (Maroto et al., 1997; Tajbakhsh et al., 1997), we think it likely that the induction of *MyoD* transcripts observed in our experiments is secondary to the induction of Pax-3/7 protein (until antibodies against chick Myf-5 become available, we cannot assess whether Wnt-3a can upregulate Myf-5 protein independent of Pax-3/7). Furthermore, if Wnt-3a were driving cells toward a myogenic fate in vivo, we would expect that the expansion of the myotome would come at the expense of the dermomyotome. However, we see an expansion of both the dermomyotome and the myotome. Another possibility is that Wnt-3a promotes the terminal differentiation of muscle cells. In this case, we would expect that an initial expansion of the myotome would be followed by a reduction in the myotome due to the premature differentiation of mitotically competent precursors. We have not observed a reduction in myotome size over the time period analyzed (0–48 h post-electroporation). Due to the transient expression of electroporated genes, we have not analyzed later time points. However, the observation that Wnt-3a causes an increase in proliferation rather than a decrease in proliferation provides solid evidence that Wnt-3a does not promote terminal differentiation.

As Pax-3 has been shown to induce proliferation (Mennerich and Braun, 2001) as well as inhibit terminal differentiation (Epstein et al., 1995) of myogenic cells, it is important to note that the observed increases in the percentage of mitotic cells in our 24-h embryos could reflect either an increase in proliferation or a delay in differentiation. While the ability of Wnt-3a to inhibit the differentiation of a subpopulation of MHC-positive cells in explant cultures is

consistent with data derived from wing bud micromass cultures (Anakwe et al., 2003), preliminary data argues for a role in proliferation. First, when explant cultures are grown in the presence of adjacent tissues, MHC protein is induced within 48 h in both the presence and absence of Wnt-3a (data not shown), suggesting that Wnt-3a does not inhibit terminal differentiation. Furthermore, the presence of differentiated cells in the myotome immediately upon its formation in Wnt-3a-treated embryos also suggests that Wnt-3a does not inhibit differentiation (data not shown). Thus, cumulatively, our data indicate that the primary role of Wnt-3a in somites is to promote proliferation.

We do not know if the increase in proliferation we are observing is general to all cells in the dermomyotome or specific for a subset of progenitor cells. Interestingly, preliminary data indicates that the myotome is expanded from the moment that it emerges from the DML (data not shown). These data are consistent with the existence of a population of mitotically competent progenitor cells in the DML (Denetclaw et al., 1997; Huang and Christ, 2000; Ordahl et al., 2001; Venters and Ordahl, 2002). If this is the case, one might expect to see that the increase in proliferation in the dermomyotome is localized to the DML; this is not observed in our experiments. However, Venters and Ordahl (2002) have shown that the dermomyotome sheet is competent to generate progenitor cells when placed in the signaling environment of the DML. By ectopically expressing Wnt-3a such that it was expressed more ventrally than endogenous Wnt-3a, we may have also expanded the region that gives rise to progenitor cells. Our data are less consonant with the notion that the primary myotome is formed by post-mitotic pioneer cells (Kahane et al., 1998) as this model does not readily explain how enhanced proliferation in the dermomyotome would cause an increase in the size of the primary myotome (unless Wnt-3a acts before these cells become post-mitotic).

In light of the recently established role of Wnt-3a in segmentation (Aulehla et al., 2003), the ability of Wnt-3a to induce proliferation at the level of the segmental plate in explant cultures is also of interest to us. It is certainly tempting to speculate that there is a link between the cell cycle clock and the segmentation clock.

The ability of purified Wnt-3a to maintain and/or induce Pax-3/7 gene and protein expression as well as proliferation in explants within 24 h provides strong evidence that these responses are indeed primary effects. However, we cannot rule out the possibility that Wnt-3a induces the explants to produce a secondary factor that then causes the observed effects. The important point is that the use of purified Wnt-3a has allowed us to rule out the possibility that non-physiologically relevant secondary factors produced by Wnt-expressing cells in the cultures were the source of the observed effects. Although data from Capdevila et al. (1998) suggest that the effects of retrovirally expressed Wnt-1 are indeed direct effects, our data from the electroporations do not directly address whether the observed effects on gene/protein expression and proliferation are primary or secondary responses to Wnt-3a. However, this is a less significant concern as it is quite possible that endogenous Wnt-3a might also act through some sort of secondary signaling relay.

Given that Wnt-1 and Wnt-3a are functionally redundant (Ikeya and Takada, 1998; Ikeya et al., 1997; Shimizu et al., 1997; Wong et al., 1994) and that ectopic expression of either Wnt-1 or activated β-catenin in somites gives a similar phenotype (Capdevila et al., 1998), we believe that Wnt-3a is likely acting through the canonical Wnt signaling pathway. We predict that our inability to detect nuclear β-catenin is a technical issue rather than an indication that Wnt-3a is utilizing an alternate signaling pathway. Investigations are ongoing to determine if β-catenin/TCF acts directly on Pax-3 and Pax-7 regulatory elements to induce transcription.

These studies have elucidated a clear proliferative role for Wnt-3a in the somite. Although we show that Wnt-3a is sufficient to expand the dermomyotome and myotome, we know that it is only required (in conjunction with Wnt-1) for the proper expansion of the medial dermomyotome (Ikeya and Takada, 1998). Thus, it seems likely that the coordinated expression and regulation of other signaling factors that promote proliferation will be required for proper expansion of the remainder of the dermomyotome.

Acknowledgments

Many thanks to Dr. Sara Venters (UCSF), Michelle Baranski (University of Washington), and Dr. Rob Welikson (University of Washington) for their critical reading of this manuscript. Thanks also to Dr. Mohammad Kafai (SFSU) for his help with the statistical analysis and Marina Meyerzon for her assistance with notochord measurements. This work was funded by NIH MBRS (SO6 GM52588) and AREA (1 R15 HD4204501) grants to LWB as well as an NIH RIMI (P20 RR11805) grant to SFSU.

References

Amthor, H., Christ, B., Patel, K., 1999. A molecular mechanism enabling continuous embryonic muscle growth—A balance between proliferation and differentiation. Development 126, 1041–1053.

Anakwe, K., Robson, L., Hadley, J., Buxton, P., Church, V., Allen, S., Hartmann, C., Harfe, B., Nohno, T., Brown, A.M., Evans, D.J., Francis-West, P., 2003. Wnt signalling regulates myogenic differentiation in the developing avian wing. Development 130, 3503–3514.

Aoyama, H., Asamoto, K., 1988. Determination of somite cells: independence of cell differentiation and morphogenesis. Development 104, 15–28.

Aulehla, A., Wehrle, C., Brand-Saberi, B., Kemler, R., Gossler, A., Kanzler, B., Herrmann, B.G., 2003. Wnt3a plays a major role in the segmentation clock controlling somitogenesis. Dev. Cell 4, 395–406.

Bader, D., Masaki, T., Fischman, D.A., 1982. Immunochemical analysis of myosin heavy chain during avian myogenesis in vivo and in vitro. J. Cell Biol. 95, 763–770.

Baranski, M., Berdougo, E., Sandler, J.S., Darnell, D.K., Burrus, L.W.,

2000. The dynamic expression pattern of frzb-1 suggests multiple roles in chick development. Dev. Biol. 217, 25–41.
Barnes, G.L., Hsu, C.W., Mariani, B.D., Tuan, R.S., 1996. Chicken Pax-1 gene: structure and expression during embryonic somite development. Differentiation 61, 13–23.
Borycki, A.G., Mendham, L., Emerson Jr., C.P., 1998. Control of somite patterning by Sonic hedgehog and its downstream signal response genes. Development 125, 777–790.
Borycki, A.G., Li, J., Jin, F., Emerson, C.P., Epstein, J.A., 1999. Pax3 functions in cell survival and in pax7 regulation. Development 126, 1665–1674.
Brand-Saberi, B., Ebensperger, C., Wilting, J., Balling, R., Christ, B., 1993. The ventralizing effect of the notochord on somite differentiation in chick embryos. Anat. Embryol. (Berlin) 188, 239–245.
Buffinger, N., Stockdale, F.E., 1994. Myogenic specification in somites: induction by axial structures. Development 120, 1443–1452.
Burrus, L.W., McMahon, A.P., 1995. Biochemical analysis of murine Wnt proteins reveals both shared and distinct properties. Exp. Cell Res. 220, 363–373.
Capdevila, J., Tabin, C., Johnson, R.L., 1998. Control of dorsoventral somite patterning by Wnt-1 and beta-catenin. Dev. Biol. 193, 182–194.
Christ, B., Ordahl, C.P., 1995. Early stages of chick somite development. Anat. Embryol. (Berlin) 191, 381–396.
Cinnamon, Y., Kahane, N., Kalcheim, C., 1999. Characterization of the early development of specific hypaxial muscles from the ventrolateral myotome. Development 126, 4305–4315.
Cossu, G., Kelly, R., Tajbakhsh, S., Di Donna, S., Vivarelli, E., Buckingham, M., 1996. Activation of different myogenic pathways: myf-5 is induced by the neural tube and MyoD by the dorsal ectoderm in mouse paraxial mesoderm. Development 122, 429–437.
Denetclaw, W.F., Ordahl, C.P., 2000. The growth of the dermomyotome and formation of early myotome lineages in thoracolumbar somites of chicken embryos. Development 127, 893–905.
Denetclaw Jr., W.F., Christ, B., Ordahl, C.P., 1997. Location and growth of epaxial myotome precursor cells. Development 124, 1601–1610.
Denetclaw Jr., W.F., Berdougo, E., Venters, S.J., Ordahl, C.P., 2001. Morphogenetic cell movements in the middle region of the dermomyotome dorsomedial lip associated with patterning and growth of the primary epaxial myotome. Development 128, 1745–1755.
Dietrich, S., Schubert, F.R., Lumsden, A., 1997. Control of dorsoventral pattern in the chick paraxial mesoderm. Development 124, 3895–3908.
Dockter, J., Ordahl, C.P., 2000. Dorsoventral axis determination in the somite: a re-examination. Development 127, 2201–2206.
Dugaiczyk, A., Haron, J.A., Stone, E.M., Dennison, O.E., Rothblum, K.N., Schwartz, R.J., 1983. Cloning and sequencing of a deoxyribonucleic acid copy of glyceraldehyde-3-phosphate dehydrogenase messenger ribonucleic acid isolated from chicken muscle. Biochemistry 22, 1605–1613.
Epstein, J.A., Lam, P., Jepeal, L., Maas, R.L., Shapiro, D.N., 1995. Pax3 inhibits myogenic differentiation of cultured myoblast cells. J. Biol. Chem. 270, 11719–11722.
Fan, C.M., Tessier-Lavigne, M., 1994. Patterning of mammalian somites by surface ectoderm and notochord: evidence for sclerotome induction by a hedgehog homolog. Cell 79, 1175–1186.
Fan, C.M., Lee, C.S., Tessier-Lavigne, M., 1997. A role for WNT proteins in induction of dermomyotome. Dev. Biol. 191, 160–165.
Gerhart, J., Baytion, M., DeLuca, S., Getts, R., Lopez, C., Niewenhuis, R., Nilsen, T., Olex, S., Weintraub, H., George-Weinstein, M., 2000. DNA dendrimers localize MyoD mRNA in presomitic tissues of the chick embryo. J. Cell Biol. 149, 825–834.
Goulding, M., Lumsden, A., Paquette, A.J., 1994. Regulation of Pax-3 expression in the dermomyotome and its role in muscle development. Development 120, 957–971.
Hamburger, V., Hamilton, H.L., 1951. A series of normal stages in the development of the chick embryo. J. Morphol. 88, 49–92.
Hendzel, M.J., Wei, Y., Mancini, M.A., Van Hooser, A., Ranalli, T., Brinkley, B.R., Bazett-Jones, D.P., Allis, C.D., 1997. Mitosis-specific phosphorylation of histone H3 initiates primarily within pericentromeric heterochromatin during G2 and spreads in an ordered fashion coincident with mitotic chromosome condensation. Chromosoma 106, 348–360.
Hirsinger, E., Duprez, D., Jouve, C., Malapert, P., Cooke, J., Pourquie, O., 1997. Noggin acts downstream of Wnt and Sonic Hedgehog to antagonize BMP4 in avian somite patterning. Development 124, 4605–4614.
Hirsinger, E., Malapert, P., Dubrulle, J., Delfini, M.C., Duprez, D., Henrique, D., Ish-Horowicz, D., Pourquie, O., 2001. Notch signalling acts in postmitotic avian myogenic cells to control MyoD activation. Development 128, 107–116.
Huang, R., Christ, B., 2000. Origin of the epaxial and hypaxial myotome in avian embryos. Anat. Embryol. (Berlin) 202, 369–374.
Ikeya, M., Takada, S., 1998. Wnt signaling from the dorsal neural tube is required for the formation of the medial dermomyotome. Development 125, 4969–4976.
Ikeya, M., Lee, S.M., Johnson, J.E., McMahon, A.P., Takada, S., 1997. Wnt signalling required for expansion of neural crest and CNS progenitors. Nature 389, 966–970.
Johnson, R.L., Laufer, E., Riddle, R.D., Tabin, C., 1994. Ectopic expression of Sonic hedgehog alters dorsal-ventral patterning of somites. Cell 79, 1165–1173.
Kahane, N., Cinnamon, Y., Kalcheim, C., 1998. The origin and fate of pioneer myotomal cells in the avian embryo. Mech. Dev. 74, 59–73.
Kawakami, A., Kimura-Kawakami, M., Nomura, T., Fujisawa, H., 1997. Distributions of PAX6 and PAX7 proteins suggest their involvement in both early and late phases of chick brain development. Mech. Dev. 66, 119–130.
Kawakami, Y., Wada, N., Nishimatsu, S., Nohno, T., 2000. Involvement of frizzled-10 in Wnt-7a signaling during chick limb development. Dev. Growth Differ. 42, 561–569.
Kenny-Mobbs, T., Thorogood, P., 1987. Autonomy of differentiation in avian branchial somites and the influence of adjacent tissues. Development 100, 449–462.
Keynes, R.J., Stern, C.D., 1988. Mechanisms of vertebrate segmentation. Development 103, 413–429.
Kiefer, J.C., Hauschka, S.D., 2001. Myf-5 is transiently expressed in non-muscle mesoderm and exhibits dynamic regional changes within the presegmented mesoderm and somites I–IV. Dev. Biol. 232, 77–90.
Maroto, M., Reshef, R., Munsterberg, A.E., Koester, S., Goulding, M., Lassar, A.B., 1997. Ectopic Pax-3 activates MyoD and Myf-5 expression in embryonic mesoderm and neural tissue. Cell 89, 139–148.
Megason, S.G., McMahon, A.P., 2002. A mitogen gradient of dorsal midline Wnts organizes growth in the CNS. Development 129, 2087–2098.
Mennerich, D., Braun, T., 2001. Activation of myogenesis by the homeobox gene Lbx1 requires cell proliferation. EMBO J. 20, 7174–7183.
Miller, S.A., 1982. Differential proliferation in morphogenesis of lateral body folds. J. Exp. Zool. 221, 205–211.
Miller, S.A., Olcott, C.W., 1989. Cell proliferation in chick oral membrane lags behind that of adjacent epithelia at the time of rupture. Anat. Rec. 223, 204–208.
Miller, S.A., Favale, A.M., Knohl, S.J., 1993. Role for differential cell proliferation in perforation and rupture of chick pharyngeal closing plates. Anat. Rec. 237, 408–414.
Miller, S.A., Bresee, K.L., Michaelson, C.L., Tyrell, D.A., 1994. Domains of differential cell proliferation and formation of amnion folds in chick embryo ectoderm. Anat. Rec. 238, 225–236.
Miller, S.A., Adornato, M., Briglin, A., Cavanaugh, M., Christian, T., Jewett, K., Michaelson, C., Monoson, T., Price, F., Tignor, J., Tyrell, D., 1999. Domains of differential cell proliferation suggest hinged folding in avian gut endoderm. Dev. Dyn. 216, 398–410.
Münsterberg, A.E., Lassar, A.B., 1995. Combinatorial signals from the neural tube, floor plate and notochord induce myogenic bHLH gene expression in the somite. Development 121, 651–660.
Münsterberg, A.E., Kitajewski, J., Bumcrot, D.A., McMahon, A.P., Lassar, A.B., 1995. Combinatorial signaling by Sonic hedgehog and Wnt family members induces myogenic bHLH gene expression in the somite. Genes Dev. 9, 2911–2922.

Nielsen, H., Engelbrecht, J., Brunak, S., von Heijne, G., 1997. Identification of prokaryotic and eukaryotic signal peptides and prediction of their cleavage sites. Protein Eng. 10, 1–6.

Ordahl, C.P., 1993. Myogenic lineages within the developing somite. In: Bernfield, M. (Ed.), Molecular Basis of Morphogenesis, 51st Annual Symposium of the Society for Developmental Biology. Wiley, New York, pp. 165–176.

Ordahl, C.P., Williams, B.A., Denetclaw, W., 2000. Determination and morphogenesis in myogenic progenitor cells: an experimental embryological approach. Curr. Top. Dev. Biol. 48, 319–367.

Ordahl, C.P., Berdougo, E., Venters, S.J., Denetclaw Jr., W.F., 2001. The dermomyotome dorsomedial lip drives growth and morphogenesis of both the primary myotome and dermomyotome epithelium. Development 128, 1731–1744.

Pownall, M.E., Strunk, K.E., Emerson Jr., C.P., 1996. Notochord signals control the transcriptional cascade of myogenic bHLH genes in somites of quail embryos. Development 122, 1475–1488.

Primmett, D.R., Norris, W.E., Carlson, G.J., Keynes, R.J., Stern, C.D., 1989. Periodic segmental anomalies induced by heat shock in the chick embryo are associated with the cell cycle. Development 105, 119–130.

Reshef, R., Maroto, M., Lassar, A.B., 1998. Regulation of dorsal somitic cell fates: BMPs and Noggin control the timing and pattern of myogenic regulator expression. Genes Dev. 12, 290–303.

Rong, P.M., Teillet, M.A., Ziller, C., Le Douarin, N.M., 1992. The neural tube/notochord complex is necessary for vertebral but not limb and body wall striated muscle differentiation. Development 115, 657–672.

Shibamoto, S., Higano, K., Takada, R., Ito, F., Takeichi, M., Takada, S., 1998. Cytoskeletal reorganization by soluble Wnt-3a protein signalling. Genes Cells 3, 659–670.

Shimizu, H., Julius, M.A., Giarre, M., Zheng, Z., Brown, A.M., Kitajewski, J., 1997. Transformation by Wnt family proteins correlates with regulation of beta-catenin. Cell Growth Differ. 8, 1349–1358.

Spence, M.S., Yip, J., Erickson, C.A., 1996. The dorsal neural tube organizes the dermamyotome and induces axial myocytes in the avian embryo. Development 122, 231–241.

Spörle, R., Gunther, T., Struwe, M., Schughart, K., 1996. Severe defects in the formation of epaxial musculature in open brain (opb) mutant mouse embryos. Development 122, 79–86.

Stern, H.M., Hauschka, S.D., 1995. Neural tube and notochord promote in vitro myogenesis in single somite explants. Dev. Biol. 167, 87–103.

Stern, H.M., Brown, A.M., Hauschka, S.D., 1995. Myogenesis in paraxial mesoderm: preferential induction by dorsal neural tube and by cells expressing Wnt-1. Development 121, 3675–3686.

Tajbakhsh, S., Rocancourt, D., Cossu, G., Buckingham, M., 1997. Redefining the genetic hierarchies controlling skeletal myogenesis: Pax-3 and Myf-5 act upstream of MyoD. Cell 89, 127–138.

Tapscott, S.J., Lassar, A.B., Davis, R.L., Weintraub, H., 1989. 5-Bromo-2′-deoxyuridine blocks myogenesis by extinguishing expression of MyoD1. Science 245, 532–536.

Venters, S.J., Ordahl, C.P., 2002. Persistent myogenic capacity of the dermomyotome dorsomedial lip and restriction of myogenic competence. Development 129, 3873–3885.

Wagner, J., Schmidt, C., Nikowits Jr., W., Christ, B., 2000. Compartmentalization of the somite and myogenesis in chick embryos are influenced by wnt expression. Dev. Biol. 228, 86–94.

Wei, Y., Yu, L., Bowen, J., Gorovsky, M.A., Allis, C.D., 1999. Phosphorylation of histone H3 is required for proper chromosome condensation and segregation. Cell 97, 99–109.

Willert, K., Brown, J.D., Danenberg, E., Duncan, A.W., Weissman, I.L., Reya, T., Yates, J.R., Nusse, R., 2003. Wnt proteins are lipid-modified and can act as stem cell growth factors. Nature 27, 27.

Williams, B.A., Ordahl, C.P., 1994. Pax-3 expression in segmental mesoderm marks early stages in myogenic cell specification. Development 120, 785–796.

Wong, G.T., Gavin, B.J., McMahon, A.P., 1994. Differential transformation of mammary epithelial cells by Wnt genes. Mol. Cell. Biol. 14, 6278–6286.

Xue, X.J., Xue, Z.G., 1996. Spatial and temporal effects of axial structures on myogenesis of developing somites. Mech. Dev. 60, 73–82.

Yablonka-Reuveni, Z., Paterson, B.M., 2001. MyoD and myogenin expression patterns in cultures of fetal and adult chicken myoblasts. J. Histochem. Cytochem. 49, 455–462.

Yamaguchi, T.P., Bradley, A., McMahon, A.P., Jones, S., 1999. A Wnt5a pathway underlies outgrowth of multiple structures in the vertebrate embryo. Development 126, 1211–1223.